

Article

A 4.7–8.8 GHz Wideband Switched Coupled Inductor VCO for Dielectric Spectroscopy Sensor

Kiho Lee ¹, Hapsah Aulia Azzahra ² , Muhammad Fakhri Mauludin ³ , Dong-Ho Lee ⁴ , Jusung Kim ^{5,*}  and Songcheol Hong ⁶ 

¹ SK Hynix, Icheon-si 17336, Republic of Korea

² Institute of Radio Frequency Engineering and Electronics, Karlsruhe Institute of Technology, 76131 Karlsruhe, Germany

³ Department of Electronics Engineering, Hanbat National University, Daejeon 34158, Republic of Korea

⁴ Department of Mobile Convergence Engineering, Hanbat National University, Daejeon 34158, Republic of Korea

⁵ Division of Electronic and Semiconductor Engineering and with the Institute for Multiscale Matter and Systems (IMMS) Laboratory, Ewha Womans University, Seoul 03760, Republic of Korea

⁶ School of Electrical Engineering, Korea Advanced Institute of Science and Technology (KAIST), Daejeon 34141, Republic of Korea

* Correspondence: jusungkim@ewha.ac.kr

Abstract

The miniaturization of dielectric sensing has driven the development of both oscillator- and receiver-based sensors. Wide-frequency-range and low-power-consumption voltage-controlled oscillators (VCOs) are required as a reference clock for receiver-based dielectric spectroscopy. In this paper, we propose a switched coupled inductor VCO offering sufficiently wide bandwidth in a power-efficient manner. The proposed switched coupled inductor offers higher coupling factor and mutual inductance compared to direct switched inductor schemes along with a higher quality factor and tuning range. The proposed switched coupled inductor improved the frequency tuning range by 21% compared to the conventional VCO. The measurement results show that the proposed VCO oscillates from 4.7 to 8.8 GHz frequency, suitable for dielectric spectroscopy sensors. With only 4.5 mW power consumption, the proposed VCO can achieve -103.3 dBc/Hz phase noise at 1 MHz offset, with a resulting tuning range figure-of-merit (FOM_T) of -187.4 dBc/Hz.

Keywords: dielectric sensing; spectroscopy; switched coupled inductor; wideband; voltage-controlled oscillator (VCO)



Academic Editors: Pengfei Gu, Jihong Gu and Tiancheng Zhang

Received: 20 December 2025

Revised: 31 December 2025

Accepted: 14 January 2026

Published: 15 January 2026

Copyright: © 2026 by the authors.

Licensee MDPI, Basel, Switzerland.

This article is an open access article distributed under the terms and conditions of the [Creative Commons Attribution \(CC BY\)](https://creativecommons.org/licenses/by/4.0/) license.

1. Introduction

The integrated circuit in biomedical devices has widely expanded. Dielectric sensing, either oscillator-based or receiver-based, has been developed to target miniaturized and self-sustained CMOS-based solutions [1]. LC voltage-controlled oscillator (VCO)-based dielectric sensing detects the permittivity of the material under test (MUT) through capacitance change, which is integrated into the VCO's LC tank within the frequency synthesizer [2]. This integration alters the VCO's free-running frequency, whose change is further translated into the control voltage of the frequency synthesizer. However, the VCO-based system can only measure the real component of the permittivity. Receiver-based sensors, on the other hand, can detect both real and imaginary component of the signal. But the RF bandwidth and the dynamic range are limited by the receiver noise and linearity.

Figure 1 depicts a current-mode, low-IF architecture for dielectric sensing. Current-domain operation eliminates the voltage-divider constraint in the signal path, removing a major source of bandwidth limitation. In addition, the adoption of a low-intermediate-frequency (low-IF) scheme effectively mitigates harmonic mixing effects, which leads to enhanced linearity and an improved dynamic range. As a result, the overall bandwidth of the sensing system is no longer dictated by the analog signal path but is instead determined by the tuning range of the reference clock generated by the frequency synthesizer [2–4]. Under this constraint, a voltage-controlled oscillator (VCO) that simultaneously offers a wide frequency tuning range and low power consumption becomes a key enabler for receiver-based dielectric sensing applications.

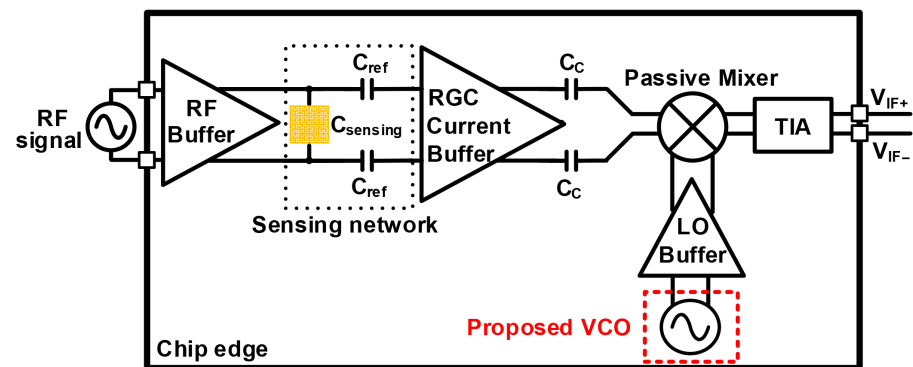


Figure 1. Current-mode low-IF receiver for dielectric sensing application.

Several methods aimed at wideband frequency tuning of VCOs, such as magnetic tuning [5,6], negative-inductance cell tuning [7], and switched coupled inductors [8,9], have been investigated. The magnetic tuning method offers wide tuning range but it significantly increases phase noise and consumes high power. Negative-inductance cell tuning provides wideband operation range by having additional cross-coupled pairs degenerated by an inductor. This cell offers tunable negative resistance and inductance by adjusting the current flow through the cell. However, the same approach does not provide wide tuning range compared to switched coupled inductors and magnetic tuning technique, and requires large silicon area due to the use of two inductors. Among those methods, switched coupled inductor technique provides lower power consumption and phase noise, while occupying a smaller area. However, the switch transistor should be carefully designed to sustain large quality factor (Q) and self-resonance frequency (SRF).

In this paper, we propose a wide-tuning (operating)-range VCO utilizing the switched coupled inductor scheme in the 28 nm CMOS process. The proposed VCO functions as the reference clock for the wideband current-mode dielectric sensing receiver depicted in Figure 1, where the wide frequency range of the reference clock is essential, along with modest jitter performance. Therefore, the open-loop VCO [10] is a more power-efficient solution than the frequency locked loop [11] if the VCO can offer sufficiently large bandwidth.

The proposed VCO in our work shows a frequency tuning range of 61%, from 4.7 to 8.8 GHz, while consuming 4.5 mW power at 1.1 V supply. which is suitable for dielectric sensing applications. The presented method offers two discrete inductance values by switching the switch transistor on and off, resulting in a 21% of frequency range improvement. The RC filter employed at the current tail provides noise filtering from the bias block and thus improves the phase noise performance of the VCO.

2. Circuit Design

Figure 2 shows the schematic of the proposed wideband VCO utilizing a switched coupled inductor. The inductor switching technique is performed as a coarse frequency tuning of the VCO; in addition, the capacitor bank and varactors are further utilized for fine frequency tuning. To improve the phase noise of the VCO, an RC low-pass filter (LPF) is applied at the tail current mirror to suppress its flicker noise contribution [12,13].

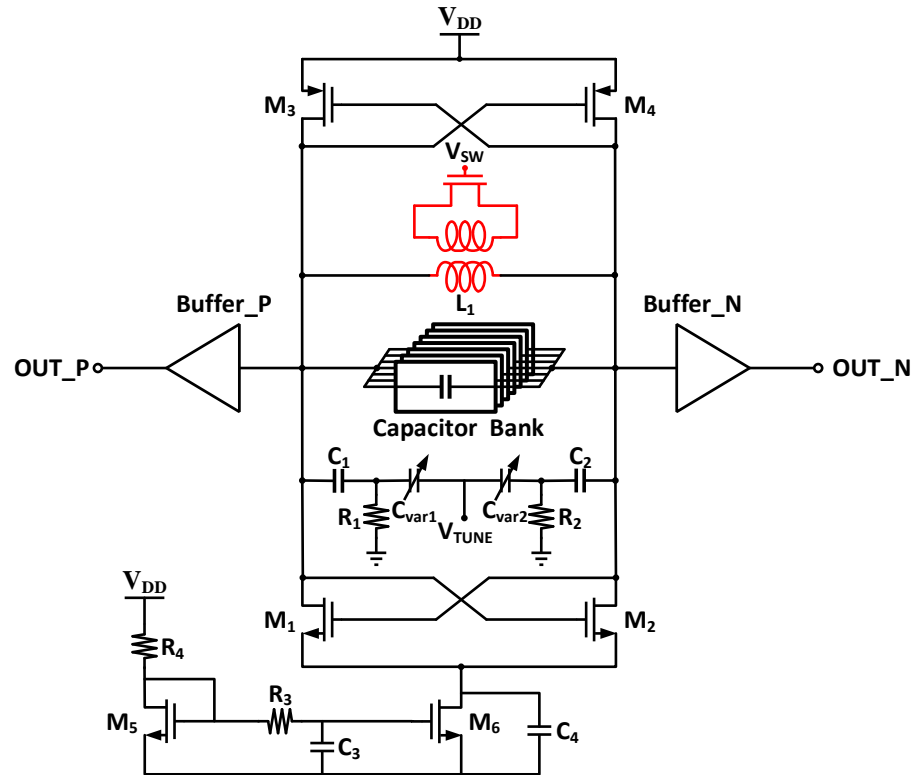


Figure 2. The proposed VCO as the reference clock of the wideband current-mode dielectric sensing receiver.

The design of the switched inductor is shown in Figure 3a. Both L_1 and L_2 are implemented with the ultra-thick metal of the technology, where it provides the smallest resistance. L_1 is a two-turn coil, and the switchable coil (L_2) is placed between the first and second turn of the L_1 coil. L_1 and L_2 are coupled through the switch transistor with mutual inductance M . Compared to [8], our method exhibits higher mutual inductance and coupling and offers a wider tuning range. Figure 3b,c show the simulated Q-factor and inductance versus frequency, respectively. To analyze the effect of the proposed switched coupled inductor scheme, a T-model of the switched coupled inductor is illustrated in Figure 4a [8]. The input impedance of the switched coupled inductor (Z_{in}) can be derived as

$$Z_{in} = j\omega L_1 + j\omega M \parallel (j\omega L_2 + Z_{SW}), \tag{1}$$

where Z_{SW} is the switch transistor impedance and M is the mutual inductance. The R_{on} and C_{off} are the representation of the switch resistance and parasitic capacitance of the transistor, whose values are meaningful for the on and off states of the transistor. When the switch transistor is turned on, Z_{SW} is approximately equal to R_{on} . Therefore, the equivalent resistance ($R_{on,eq}$) and inductance ($L_{on,eq}$) are given by

$$R_{on,eq} = \frac{-\omega^2 L_2 M R_{on} + \omega^2 M (L_2 + M) R_{on}}{R_{on}^2 + \omega^2 (L_2 + M)^2} \tag{2}$$

$$L_{on,eq} = L_1 + \frac{MR_{on}^2 - \omega^2 L_2 M(L_2 + M)}{R_{on}^2 + \omega^2(L_2 + M)^2} \tag{3}$$

Assuming that $R_{on} \ll \omega(L_2 + M)$, $R_{on,eq}$ and $L_{on,eq}$ can be written as

$$R_{on,eq} \approx \left(\frac{M}{L_2 + M}\right)^2 R_{on} \tag{4}$$

$$L_{on,eq} \approx L_1 - \frac{L_2 M}{L_2 + M} \tag{5}$$

As can be seen in (5), the inductance is reduced by $L_2 M / (L_2 + M)$ when the switch is on, and it provides the desired coarse tuning function of the LC tank. Furthermore, switched coupled inductor method gives smaller effective resistance, as depicted in (4), compared to the on state of the direct switched inductor in Figure 4b, which gives $R_{on,eq} = \omega^2 L_b^2 R_{on} / (R_{on}^2 + \omega^2 L_b^2) \approx R_{on}$. Thus, the switched coupled inductor provides higher Q-factor.

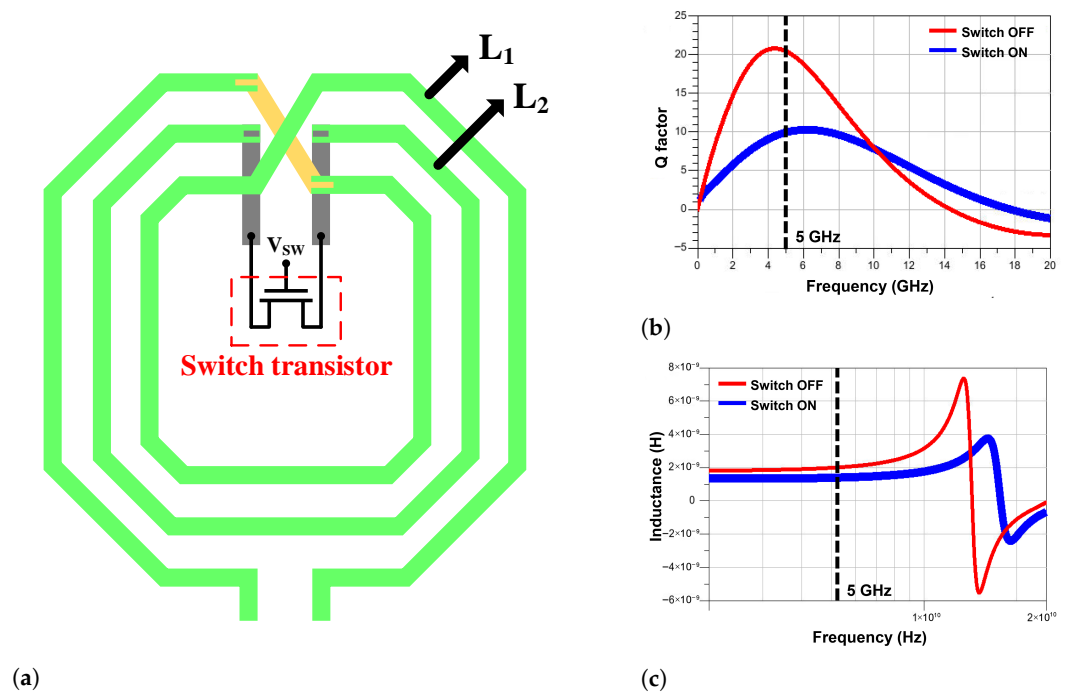


Figure 3. (a) Switched coupled inductor design, (b) simulated Q-factor, and (c) inductance.

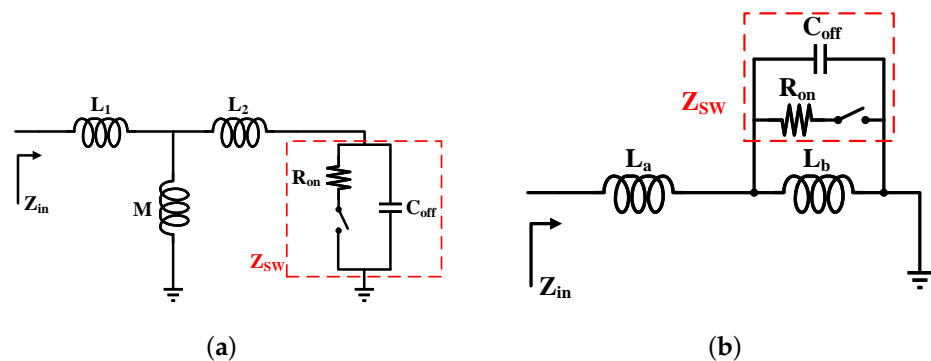


Figure 4. Comparison of (a) switched coupled inductor and (b) direct switched inductor.

A key design trade-off in a switched coupled inductor lies in the sizing of the switch transistor. Enlarging the switch reduces its on-state resistance, which in turn enhances the

effective quality factor when the switch is activated. However, this benefit comes at the expense of a reduced self-resonance frequency (SRF) for the overall inductor structure due to increased parasitic capacitance. Figure 5 presents simulated variations in the inductance and quality factor as a function of switch transistor width. As the transistor width is swept from 50 to 500 μm , an optimal point emerges that simultaneously satisfies both high-Q and high-SRF requirements. Based on these results, a switch width of 300 μm is selected, as it achieves a quality factor exceeding 10 while maintaining an SRF above 15 GHz. For the chosen configuration, the extracted mutual inductance and effective coupling coefficient are

$$M = 0.85 \text{ nH} \tag{6}$$

$$K = 0.43. \tag{7}$$

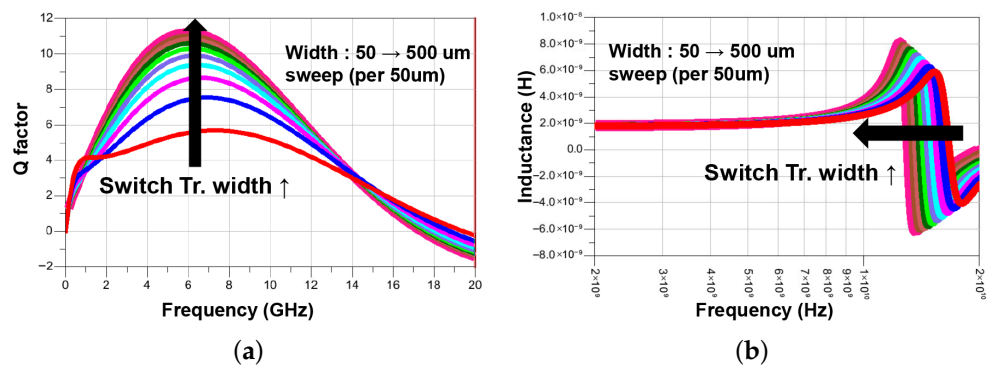


Figure 5. The effect of switch transistor size on (a) Q-factor and (b) inductance.

3. Measurement Result

The proposed switched coupled inductor VCO is implemented using a Samsung bulk 28 nm CMOS process. The total chip area is $644 \mu\text{m} \times 750 \mu\text{m}$ with the core area of $292 \mu\text{m} \times 453 \mu\text{m}$, as shown in Figure 6a. Our proposed VCO is equipped with 4-bit digital control (0 to 15), where we use the code from 0 to 8 only for our measurement. A diagram of the measurement setup is illustrated in Figure 6b. The differential VCO output is converted to a single-ended signal using an off-chip balun (mini-circuit, SCTX2-93-2W) and then measured by a PXA Signal Analyzer N9030A. The chip consumed 4.5 mW power from a 1.1 V supply voltage.

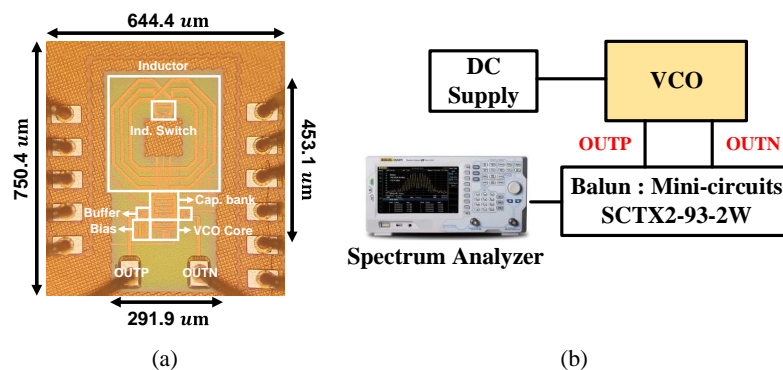


Figure 6. (a) Chip micrograph and (b) measurement setup.

Figure 7 shows the measured frequency spectrum at 5.63 GHz when inductor switch is off, with -23.56 dBm output power. The output was measured directly through the balun (off-chip) and spectrum analyzer. The loss due to the balun is not de-embedded since it merely shifts the output power level. The unmatched output connection is manifested by

the different output power levels across the tuning range. However, this is not a limitation of our design.

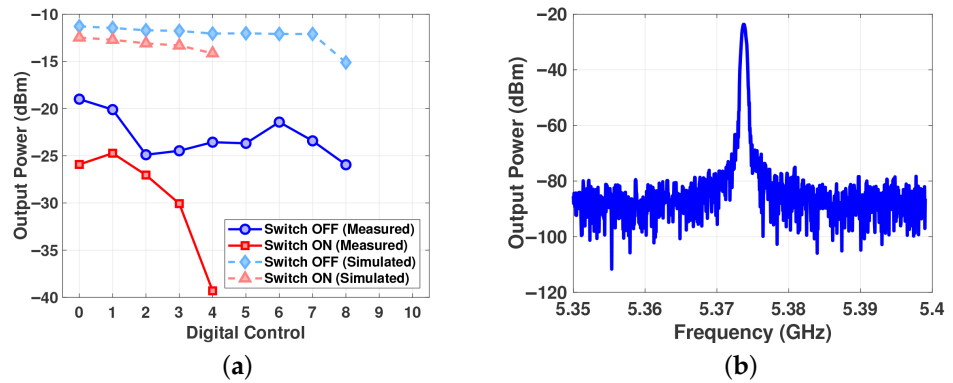


Figure 7. (a) Measured and simulated VCO's output power and (b) measured spectrum of VCO, oscillating at 5.63 GHz.

When the switch transistor is in the off state, the frequency range is 4.7 to 7.26 GHz (42%) with different digital control settings. When the switch is on, the frequency range is 6.46 to 8.8 GHz, which provides additional 21% tuning range. Note that the Q -factor of the inductor in the on state is smaller than in the off state, so the bearable digital control of the capacitor bank is up to 4. The measured overall frequency range of the VCO is 4.7–8.8 GHz (61% tuning range), as shown in Figure 8. Moreover, Figure 9 illustrates the fine tuning frequency by changing the bias voltage (V_{tune}) of the varactors when the inductor switch is off and the digital control of the capacitor bank is completely off.

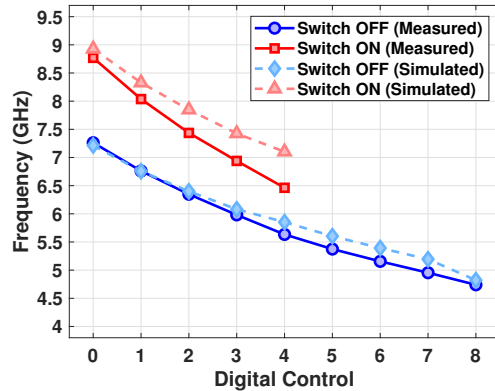


Figure 8. VCO frequency with coarse tuning inductor.

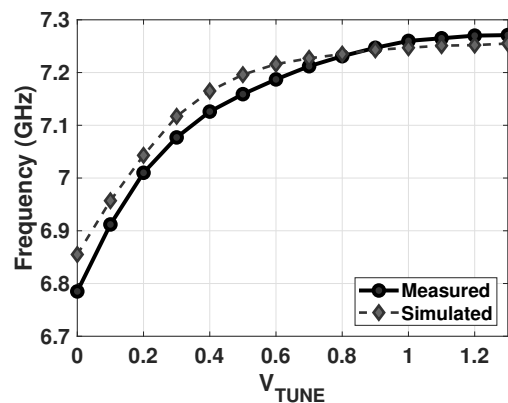


Figure 9. Measured VCO frequency with fine tuning varactor at digital switch 0.

Figure 10a shows measured phase noise at the same oscillation frequency of 5.63 GHz. The phase noise at 10 kHz and 1 MHz frequency offset along the VCO frequency range is depicted in Figure 10b. Generally, the phase noise for both frequency offsets is higher when the switch is turned on due to lower Q-factor. The best phase noise at 1 MHz is achieved at 5.63 GHz, which gives -103.3 dBc/Hz phase noise.

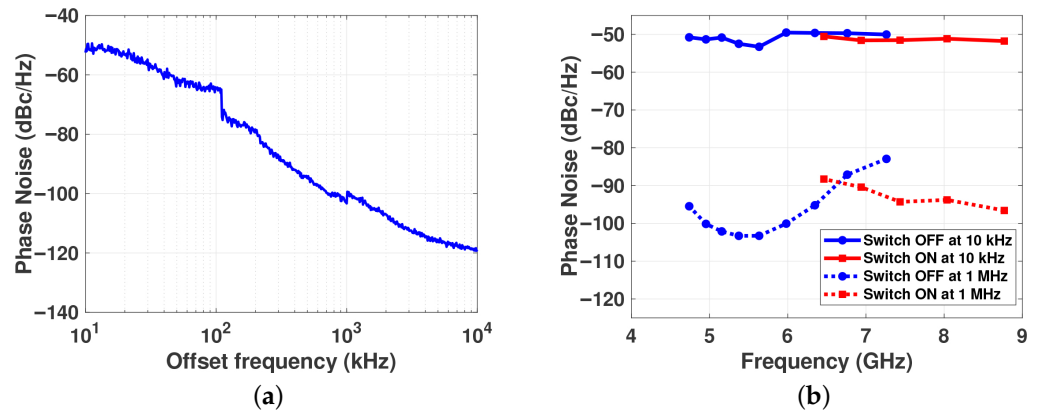


Figure 10. Measured VCO phase noise (a) at 5.63 GHz oscillation frequency and (b) at 10 kHz and 1 MHz offset at different frequencies.

To compare the overall VCO performance, figure-of-merit (FOM_T), defined in [7], is used as shown below:

$$FOM_T = L(\Delta\omega) - 20 \log \frac{\omega_0}{\Delta\omega} + 10 \log \frac{P_{DC}}{1mW} - 20 \log \frac{FTR}{10}, \quad (8)$$

where $L(\Delta\omega)$ is the phase noise at offset frequency $\Delta\omega$, ω_0 is the oscillation frequency, P_{DC} is power consumption, and FTR is frequency tuning range. The proposed VCO achieves -187.4 dBc/Hz FOM_T . Table 1 shows the performance comparison of the proposed VCO with previous works. Compared to conventional VCO without the switched coupled inductor in [14], the proposed VCO can improve frequency tuning range by 21%. Compared to the same switched coupled inductor in [8], which uses two inductor switches, our work can achieve 61% tuning range with only one inductor switch. Furthermore, it shows that the proposed one has wider frequency tuning range and lower power consumption compared to other works.

Table 1. Performance comparison of proposed VCO with published results.

	[8]	[7]	[14]	[15]	This Work
FTR (GHz)	8.05–15.32 (62%)	3.8–5.2 (31%)	4.6–6.7 (39%)	4.5–7.1 (45%)	4.74–8.77 (61%)
P_{DC} (mW)	7.67	6.4–20.2	4.35	14	4.5
PN (dBc/Hz) @1 MHz	-104	-110	-105	-109	-103.3
FOM_T	-192.4	-186	-184	-185.1	-187.4
Topology	Switched Coupled Inductor	Tunable Negative Inductance	Capacitor Bank	CM Feedback Diff. Inductor	Switched Coupled Inductor
Technology	90 nm CMOS	0.35 μ m BiCMOS	28 nm CMOS	90 nm CMOS	28 nm CMOS

4. Conclusions

In this paper, a switched coupled inductor VCO is proposed and implemented using a Samsung bulk 28 nm CMOS process. The switched inductor technique significantly improves the tuning range by 21%. The careful design methodology for the switch transistor

provides a high Q -factor and large SRF at the same time. The VCO performance is calculated using FOM_T and is found to be -187.4 dBc/Hz.

Author Contributions: Conceptualization, K.L. and S.H.; methodology, K.L.; formal analysis, K.L. and S.H.; writing—original draft preparation, H.A.A.; writing—review and editing, M.F.M. and J.K.; supervision, J.K., D.-H.L., and S.H.; funding acquisition, J.K. All authors have read and agreed to the published version of the manuscript.

Funding: This work was supported in part by the Basic Science Research Program through NRF funded by MOE under Grant 2021R111A304418211, in part by the National Research Foundation (NRF) grant funded by the Korean Government (MSIT) under Grant RS-2025-00516839 and Grant RS-2025-02217987, and also supported by the NRF grant funded by the Korea government (MSIT and MOE) (No. RS-2025-16063688).

Data Availability Statement: Data are contained within the article.

Acknowledgments: The EDA tool was supported by the IC Design Education Center.

Conflicts of Interest: Kiho Lee was employed by the company SK Hynix. The remaining authors declare that the research was conducted in the absence of any commercial or financial relationships that could be construed as a potential conflict of interest.

References

1. Entesari, K.; Helmy, A.A.; Moslehi-Bajestan, M. Integrated Systems for Biomedical Applications: Silicon-Based RF-Microwave Dielectric Spectroscopy and Sensing. *IEEE Microw. Mag.* **2017**, *18*, 57–72. [[CrossRef](#)]
2. Helmy, A.A.; Jeon, H.J.; Lo, Y.C.; Larsson, A.J.; Kulkarni, R.; Kim, J.; Silva-Martinez, J.; Entesari, K. A Self-Sustained CMOS Microwave Chemical Sensor Using a Frequency Synthesizer. *IEEE J. Solid-State Circuits* **2012**, *47*, 2467–2483. [[CrossRef](#)]
3. Chien, J.C.; Niknejad, A.M. Oscillator-Based Reactance Sensors with Injection Locking for High-Throughput Flow Cytometry Using Microwave Dielectric Spectroscopy. *IEEE J. Solid-State Circuits* **2016**, *51*, 457–472. [[CrossRef](#)]
4. Elkholy, M.; Entesari, K. A Wideband Low-Power LC-DCO-Based Complex Dielectric Spectroscopy System in 0.18- μ m CMOS. *IEEE Trans. Microw. Theory Tech.* **2017**, *65*, 4461–4474. [[CrossRef](#)]
5. Wang, K.; Tang, R.; Zhao, Z.; Zhang, J.; Li, D.; Geng, L.; Gui, X. A Low Gain Variation LC-VCO With Mutual Inductive Tuning for K_{vco} Linearity Compensation. *IEEE Microw. Wirel. Technol. Lett.* **2023**, *33*, 55–58. [[CrossRef](#)]
6. Cusmai, G.; Repossi, M.; Albasini, G.; Svelto, F. A 3.2-to-7.3 GHz Quadrature Oscillator with Magnetic Tuning. In Proceedings of the 2007 IEEE International Solid-State Circuits Conference. Digest of Technical Papers, San Francisco, CA, USA, 11–15 February 2007; pp. 92–589. [[CrossRef](#)]
7. Chen, Y.; Mouthaan, K. Wideband Varactorless LC VCO Using a Tunable Negative-Inductance Cell. *IEEE Trans. Circuits Syst. I Regul. Pap.* **2010**, *57*, 2609–2617. [[CrossRef](#)]
8. Demirkan, M.; Bruss, S.P.; Spencer, R.R. Design of Wide Tuning-Range CMOS VCOs Using Switched Coupled-Inductors. *IEEE J. Solid-State Circuits* **2008**, *43*, 1156–1163. [[CrossRef](#)]
9. Demirkan, M.; Bruss, S.P.; Spencer, R.R. 11.8GHz CMOS VCO with 62% Tuning Range Using Switched Coupled Inductors. In Proceedings of the 2007 IEEE Radio Frequency Integrated Circuits (RFIC) Symposium, Honolulu, HI, USA, 3–5 June 2007; pp. 401–404. [[CrossRef](#)]
10. McCorquodale, M.S.; O'Day, J.D.; Pernia, S.M.; Carichner, G.A.; Kubba, S.; Brown, R.B. A Monolithic and Self-Referenced RF LC Clock Generator Compliant with USB 2.0. *IEEE J. Solid-State Circuits* **2007**, *42*, 385–399. [[CrossRef](#)]
11. Elhadidy, O.; Shakib, S.; Krennek, K.; Palermo, S.; Entesari, K. A Wide-Band Fully-Integrated CMOS Ring-Oscillator PLL-Based Complex Dielectric Spectroscopy System. *IEEE Trans. Circuits Syst. I Regul. Pap.* **2015**, *62*, 1940–1949. [[CrossRef](#)]
12. Ismail, A.; Abidi, A. CMOS differential LC oscillator with suppressed up-converted flicker noise. In Proceedings of the 2003 IEEE International Solid-State Circuits Conference, San Francisco, CA, USA, 13 February 2003; Digest of Technical Papers; Volume 1, pp. 98–99. [[CrossRef](#)]
13. Tchamov, N.N.; Tchamov, N.T. Technique for Flicker Noise Up-Conversion Suppression in Differential LC Oscillators. *IEEE Trans. Circuits Syst. II Express Briefs* **2007**, *54*, 959–963. [[CrossRef](#)]

14. Lee, K.; Lee, D.; Kim, J.; Hong, S. Wideband LC VCO with 39.3 % Frequency Tuning Range for Dielectric Spectroscopy System. In Proceedings of the 2021 18th International SoC Design Conference (ISOCC), Jeju Island, Republic of Korea, 6–9 October 2021; pp. 39–40. [[CrossRef](#)]
15. Soltanian, B.; Ainspan, H.; Rhee, W.; Friedman, D.; Kinget, P.R. An Ultra-Compact Differentially Tuned 6-GHz CMOS LC-VCO with Dynamic Common-Mode Feedback. *IEEE J. Solid-State Circuits* **2007**, *42*, 1635–1641. [[CrossRef](#)]

Disclaimer/Publisher’s Note: The statements, opinions and data contained in all publications are solely those of the individual author(s) and contributor(s) and not of MDPI and/or the editor(s). MDPI and/or the editor(s) disclaim responsibility for any injury to people or property resulting from any ideas, methods, instructions or products referred to in the content.